J. Physiol. (1985), **367**, *pp.* 267–290
With 14 *text-figures*
Printed in Great Britain

MEMBRANE VOLTAGE, RESISTANCE, AND CHANNEL SWITCHING IN ISOLATED MOUSE FIBROBLASTS (L CELLS): A PATCH-ELECTRODE ANALYSIS

BY SHIGERU HOSOI AND CLIFFORD L. SLAYMAN

From the Department of Physiology, Yale School of Medicine, 333 Cedar Street, New Haven, CT 06510, U.S.A.

(*Received 22 August 1984*)

SUMMARY

1. The whole-cell patch-electrode technique of Fenwick, Marty & Neher (1982) has been applied to single suspension-cultured mouse fibroblasts. Seals in the range of 10–50 GΩ were obtained without special cleaning of the cell membranes.

2. Rupture of the membrane patch inside the electrode was accompanied by a shift of measured potential into the range −10 to −25 mV, but in most cases with little change in the recorded resistance. The latter fact implied that (i) the absolute resistance of the cell membrane must be in the same range as the seal resistance and (ii) the recorded potential is a poor measure of actual cell membrane potential.

3. Steady-state current–voltage curves (range −160 mV to +80 mV) were generated before and after rupture of the membrane patch, and the difference between these gave (zero-current) membrane potentials of −50 to −75 mV, which represents a leak-corrected estimate of the true cell-membrane potential.

4. The associated slope conductivity of the cell membrane was 5–15 μS/cm^2 (assumed smooth-sphere geometry, cells 13–15 μm in diameter) and was K^+-dominated.

5. With 0·1 mM (or more) free Ca^{2+} filling the patch electrode, membrane potentials in the range −60 to −85 mV were observed following patch rupture, with associated slope conductivities of 200–400 μS/cm^2, also K^+-dominated.

6. Similar voltages and conductivities were observed at the peak of pulse-induced 'hyperpolarizing activation' (Nelson, Peacock, & Minna, 1972), and the two phenomena probably reflect the behaviour of Ca^{2+}-activated K^+ channels.

7. Both the pulse-induced conductance and the Ca^{2+}-activated conductance spontaneously decayed, the latter over periods of 5–15 min following patch rupture.

8. Sr^{2+}, Ba^{2+}, and Co^{2+} could also activate the putative K^+ channels, but only Sr^{2+} really mimicked Ca^{2+}. Co^{2+} and Ba^{2+} activated with a delay of several minutes following patch rupture, and deactivated quickly with a small decrease of conductance and a large decrease of membrane potential. Evidently, Co^{2+} and Ba^{2+} affect channel specificity as well as channel opening and closing kinetics.

INTRODUCTION

Recording techniques. The use of intracellular glass microcapillary electrodes for study of transmembrane potential differences (Osterhout (1925) for giant algal cells, Ling & Gerard (1949) for muscle and nerve), opened up a wide range of preparations for direct study of bioelectric phenomena: in secretion, in energy distribution and in energy conservation, as well as in excitability. Furthermore, over the past 10 years the use of ultrafine microcapillaries (tip diameters of 0·05–0·2 μm: Brown & Flaming, 1977) has spread to a variety of unexpectedly small cells, including insect optic cells (Jensen & DeVoe, 1983), isolated cultured cells (Sherbet, 1978), small plant cells (Etherton, Keifer & Spanswick, 1977; Bates, Goldsmith & Goldsmith, 1982), fungal spheroplasts (Blatt & Slayman, 1983), and even certain bacteria (Felle, Stetson, Long & Slayman, 1979). At the same time, however, limitations of the microcapillary technique have become glaringly obvious: finite sealing resistances and flooding of cell cytoplasm with spurious salt can easily falsify all of the apparent electrical paramenters of punctured cells (Lassen, 1977; Nelson, Ehrenfeld & Lindemann, 1978; Page, Kelday & Bowling, 1981; Fromm & Schultz, 1981; Blatt & Slayman, 1983).

A major improvement in technique was afforded by the recent remarkable discovery (Hamill, Marty, Neher, Sakmann & Sigworth, 1981) that blunt microcapillaries (tip diameters 0·5–1·0 μm) applied firmly to the *outsides* of clean cell membranes could seal with resistances as high as 10^{11} Ω, compared with less than 5×10^9 Ω for penetrating electrodes (Lindemann, 1975; C. L. Slayman, unpublished experiments). When such an electrode is filled with a saline solution resembling cytoplasm, rather than the usual 'bridge' salt, stable recordings can be obtained from very small cells, after the membrane patch sealed into the electrode is broken (whole-cell recording mode (Fenwick, Marty & Neher, 1982; Marty & Neher, 1984)).

In fact, the whole-cell patch-electrode technique can offer not only a better method of recording from small cells, but also a direct way of evaluating the contribution which the electrode sealing junction makes to recorded voltage and resistance. The latter is possible when the resistance of the sealed-in patch of membrane is much larger than the sealing junction itself (i.e. $\gg 10^{11}$ Ω; but see Fenwick *et al.* 1982). Then current–voltage (I–V) measurements made over a wide voltage span describe both the resistance and the voltage of the junction, whether or not the seal is electrically linear.

Cultured cells. Because of the rapidly expanding interest in transport properties of cultured cells, and the hypothesis that membrane electrical events may play an important role in growth and development (Liboff & Rinaldi, 1974), we have decided to re-examine the properties of certain cultured-cell membranes using the patch-electrode technique. Mouse-embryo fibroblasts (L cells) have been selected because of three curious properties: (i) low resting membrane potentials, *ca.* −15 mV (Lamb & MacKinnon, 1971*b*; Nelson, Peacock & Minna, 1972; Okada, Doita, Roy, Tsuchiya, Inouye & Inouye, 1977); (ii) reported membrane resistances (absolute) which appear to be independent of cell size (Okada *et al.* 1977); (iii) conspicuous hyperpolarizing swings of potential associated with activation of Ca^{2+}-dependent K^+ channels (hyperpolarizing activation, or hyperpolarizing response (h.a.); Henkart & Nelson, 1979; Okada, Tsuchiya & Inouye, 1979).

By means of whole-cell patch-electrode recording, applied to normal suspension-cultured L cells, we have demonstrated resting membrane potentials in the range of -50 to -75 mV, which are elevated only slightly during h.a. Under both resting and h.a. conditions the L-cell membrane is dominated by K^+, but the absolute conductance for K^+ is about 50-fold larger in h.a. than at rest.

METHODS

Cell line and conditions of growth and recording. Suspension cultures of the mouse fibroblastic line LM(TK^-), a thymine-kinase-deficient strain of L cells (Sanford, Earle & Likely, 1948) were mainly used throughout these experiments. Starter suspensions were obtained by detaching cells from stationary cultures with 0·15% (w/v) trypsin in α medium (Stanners, Eliceiri & Green, 1971) and inoculating at 10^5 cells/ml into spinner bottles containing α medium supplemented with 5% (v/v) horse serum, in a humidified atmosphere of 5% CO_2/95% air, at 37 °C (Jayme, Adelberg & Slayman, 1981). Cell densities were maintained near 5×10^5/ml by diluting the cultures with fresh medium every 2–3 days. Cells used for most electrical recording were spherical, with normal diameters of 13–15 μm. In experiments with outside-out patches, however, attached cells were prepared by pre-incubating a drop of cell suspension on an acid-cleaned glass cover-slip for 12 h at 37 °C and 100% humidity. The electrical experiments themselves were carried out at ambient temperatures (21–24 °C).

The recording chamber consisted of a glass microscope slide 2·5 × 4·0 cm glued to the bottom of a Lucite spacer 3 mm thick and shaped to fit the mechanical stage of a phase-contrast microscope (American Optical Co. Phase-Star, Model One-Ten). The chamber was partially closed on top by a no. 1 glass cover-slip 0·5 × 1·8 cm, with slots at the front and back left open for the electrodes and for pipettes to feed and withdraw solution. The chamber had a total volume of 0·6 ml and was filled with recording medium (see below) prior to the start of each experiment. Cells were added to the bottom of the chamber in a 10 μl droplet and allowed to settle for 10–15 min, after which many cells had stuck lightly to the chamber bottom. Slow perfusion (0·5–1·0 ml/min) of the chamber was then initiated with buffered saline solution, which usually contained 10 mM-*N*-2-hydroxyethyl-piperazine-*N'*-2-ethanesulphonic acid (HEPES) brought to pH 7·2–7·3 with ~ 4 mM-NaOH, plus 160 mM-NaCl, 6 mM-KCl, 2 mM-$CaCl_2$, 1 mM-$MgCl_2$ and 0·25 mM-K_2HPO_4 (Standard Bathing Medium, SBM). High-K^+ perfusion solutions were obtained by substituting KCl for part or all of the NaCl in SBM. For rapid changes of solution in the surround of a particular cell, either the desired solution was expelled onto the cell by means of an extracellular supply needle (18-gauge syringe) placed very nearby, or the patch electrode, with cell attached, was inserted into the supply needle (Yellen, 1982). With practice, both of these manoeuvres could be executed without disturbing the patch seal.

The standard solution for filling the patch pipette resembled SBM, but contained no NaCl, K_2HPO_4, or $CaCl_2$, and had 150 mM-KCl. In some experiments, 75 mM-K_2SO_4 was substituted for the KCl in order to control for Cl^- conductance, and in most experiments Ca^{2+} and/or EGTA were added to control intracellular free Ca^{2+}. EGTA at 2·1 mM and total Ca^{2+} at 2·0 mM, 1·0, 0·2, and 0 (< 10 μM) give free Ca^{2+} concentrations of 10^{-6}, 10^{-7}, 10^{-8} and $< 10^{-9}$ M free Ca^{2+}, respectively (see Caldwell, 1970). Patch pipettes were filled at ambient temperature and pressure by direct capillarity at the tip, followed by back-filling via a fine syringe needle.

Recording and analysis. The patch-clamp amplifier used throughout these experiments was developed by Dr D. P. Corey and Mr V. Pantani in the Yale Department of Physiology. The voltage- or current-clamp mode (see schematic diagram in Fig. 1 *A*) and clamping program could be set either manually or by computer, and in the present experiments *I–V* data were obtained via a bipolar staircase of voltage-clamp pulses of 100 ms duration and clamp-charging times of less than 30 ms (depending on several factors such as the extent of Sylgard coating, capacitance compensation, clamping voltage, or the area of the pipette immersed into the solution). Sample-and-hold windows were read in the last 10 ms of each pulse, so the *I–V* curves obtained must be considered electrical steady-state relationships. A North Star Horizon II microcomputer (North Star Computer Co., San Leandro, CA, U.S.A.) was interfaced with the amplifier via Tecmar AD and DA boards (nos. TM AD-100 and TM DA-100; Tecmar, Inc., Cleveland OH, U.S.A.). Time courses of voltage and current were recorded with a FM recording adaptor (frequency response from d.c. to 1000 Hz

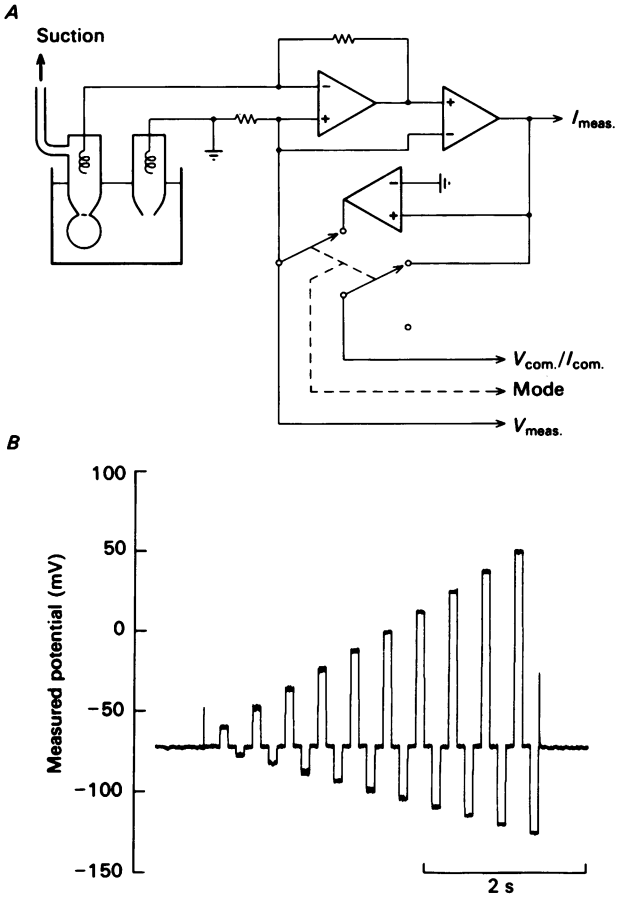

Fig. 1. Measuring arrangements for whole-cell patch-electrode experiments. *A*, a simplified drawing of the recording circuit; the command voltage and the clamp-mode switch were controlled by computer. *B*, stimulus wave form for a typical voltage-clamp scan in the whole-cell mode, recorded on a FM tape system, after the zero-current potential was determined, voltage at the tip of the patch pipette was clamped by a series of alternating pulses, from about −100 to +80 mV. Although the traces shown are broadened by FM noise, the intrinsic voltage noise at the amplifier output (which was sampled directly by the computer) was 0·1 mV, over the frequency range 0–500 Hz. Meas., measured; com., command.

without ringing; Model 2D, A. R. Vetter Co., Rebersburg, PA, U.S.A.) and an audio cassette deck (Model AD-F660U, Aiwa America Inc., Moonachine, NJ, U.S.A.). Operation of the recording system was controlled by computer via one parallel port. Records thus obtained were played back through low-pass Butterworth filters (500 Hz cut-off frequency), digitized at a sampling frequency of 1 kHz, and displayed on an *X–Y* plotter (Model DP-10, Houston Instrument, Austin, TX, U.S.A.).

Whole-cell recording with the patch electrode was performed as described by Hamill *et al.* (1981) and Fenwick *et al.* (1982), by means of fire-polished micropipettes having $< 1{\cdot}0$ μm inside diameter and 3–8 MΩ open-tip resistances (when filled with 150 mM-KCl and dipped into SBM). Gigohm seals were established by gentle suction on the L-cell membranes, without prior enzymatic treatment. In most cases the transition from cell-attached patch recording, to whole-cell recording was achieved by breaking the sealed-in patch with a strong suction pulse after the gigohm seal had formed (see rapid fall of traces in Figs. 6 and 8).

The recording circuit assumed for analysis is shown in Fig. 2*A*. It contains three large resistances: r_p (patch), expected to be about 10^{12} Ω, when no channel is detectable; r_s (seal), observed on average near 2×10^{10} Ω; and r_m (whole membrane), expected in the range 10^8–10^{10} Ω. It also contains three smaller resistances: r_e (patch electrode), r_c (cytoplasm), and r_r (reference electrode), which are $\ll 10^7$ Ω and can be neglected. Of the six distinct e.m.f.s included, E_p and E_m represent the local (patch) and whole-cell membrane, respectively, while E_r (reference electrode), E_s (seal), E_e (bridge inside the patch pipette) and E_c (interface between cytoplasm and the pipette solution) represent liquid junction potentials. Although the resistances in series with the cell membrane (r_e, r_c and r_r)

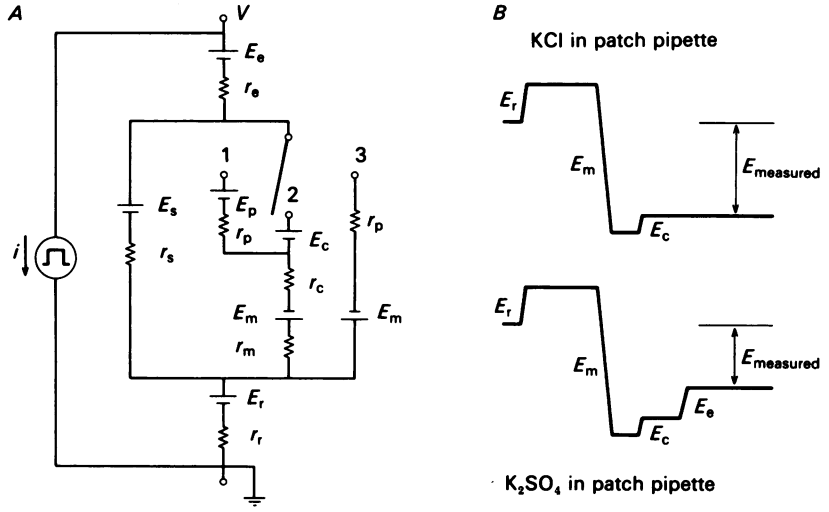

Fig. 2. *A*, diagram of the membrane circuit associated with patch-electrode recording. Subscript key: p = patch membrane; m = whole-cell membrane; s = glass-to-membrane seal; e = patch electrode; c = cytoplasm; r = reference electrode and bathing medium. The size ordering of expected resistances in the circuit is as follows: $r_p \gg r_m$, $r_s \gg r_c$, r_r, r_e. *B*, relation of the actual membrane potential to the measured potential difference, as corrected by three juction potentials (E_r, E_e, E_c), depending on whether identical (upper diagram) or non-identical (lower diagram) solutions are used in the reference and patch pipettes.

may be assumed to be negligible, the corresponding liquid junction potentials cannot necessarily be ignored. In the standard recording conditions, both the reference (bath) and recording (patch) pipettes contained 150 mM-KCl and were connected to the amplifier via KCl–agar bridges and matched Ag–AgCl half-cells. The potential E_c, expected in the whole-cell recording mode, has been estimated to be approximately 10 mV (Marty & Neher, 1984), and should decline with time as cytoplasm and pipette solution mix. In the present study, no correction has been made for E_c. E_r, the potential between the reference electrode and the bath solution, was measured by inserting a plug of agar–3 M-KCl to eliminate junction potentials between the bath and the agar bridge of the patch electrode. Its value, 4·5 mV, must be added to the measured voltage in order to obtain the transmembrane potential difference (upper diagram, Fig. 2*B*). When the patch pipette contained 75 mM-K_2SO_4 (instead of 150 mM-KCl), E_e was found to be 5·8 mV, and that likewise was added to the measured potential (see lower diagram, Fig. 2*B*). (In the text which follows, the term 'membrane potential' is reserved for the open-circuit potential adjusted for all the above corrections; measured or 'zero-current potential', used generally in the text, does not include the corrections.)

Except for adjustments required because of liquid junction potentials, correction of membrane electrical measurements for current leakage through the membrane-to-glass seals was carried out by subtracting the control *I–V* relationship obtained before patch rupture (or after outside-out

patch formation) from successive 'test' I–V curves obtained after patch rupture. This procedure arose from the following circuit considerations derived from Fig. 2*A*. With the patch electrode attached to the cell and the patch membrane intact (switch position 1), $r_p \gg r_s$, r_m, and the measured I–V relationship characterizes mainly the left branch (elements E_s and r_s) plus the series elements E_r, r_r, E_e and r_e:

$$i_1 = \frac{(V_1 - E_r - E_e)\, r_p - (E_p + E_m)\, r_s - E_s r_p}{r_s r_p}. \tag{1}$$

On the other hand, with the patch membrane broken (switch position 2), appreciable currents flow through both the seal (E_s, r_s) and the whole-cell membrane (E_m, r_m):

$$i_2 = \frac{(V_2 - E_r - E_e)\, (r_s + r_m) - (E_c + E_m)\, r_s - E_s r_m}{r_s r_m}. \tag{2}$$

Finally, if the seal is stable, so that current through it does not change, either with time or as a consequence of breaking the membrane patch, then the I–V curve for the whole-cell membrane is given by the difference, $i_2 - i_1$:

$$i_m = \frac{V - (E_m + E_c + E_r + E_e)}{r_m} + \frac{E_p + E_m}{r_p} \tag{3.1}$$

$$\simeq \frac{V - (E_m + E_c + E_r + E_e)}{r_m}, \tag{3.2}$$

in which the currents i_1 and i_2 are obtained at equal voltages, $V_1 = V_2 = V$, before and after breaking of the membrane patch. Expression (3.2) also gives the seal-corrected membrane current when comparison is made between outside-out patches (position 3) and whole-cell records (position 2).

The argument leading from eqns. 1 and 2 to eqns. (3.1) and (3.2) depends on two assumptions: (i) that $r_p \gg r_s$, and (ii) that r_s is constant during changes of the patch/cell configuration. Evidence is presented later (see Fig. 5 and the adjoining discussion) that these assumptions do hold in most cases.

However, because in practice the I–V data were somewhat noisy, subtraction of one curve from another required smoothing of the data, which was accomplished by fitting each I–V point-plot with a polynomial equation. Ordinary polynomials of degree 2, up to degree 5 (depending on a visual assessment of curve shape) were used, and least-squares fits were obtained via the Marquardt algorithm (Marquardt, 1963). Curve subtraction was then accomplished analytically rather than graphically. The over-all procedure is demonstrated in Figs. 3 and 4; the I–V plots and smoothed curves are shown in Fig. 3, and the difference I–V curves for the same experiment are shown in Fig. 4.

In all cases, the polynomial fits to I–V data were very good; so for simplicity in representation, most results after Figs. 3 and 4 have been displayed as fitted polynomials, rather than as plotted data points. All primary data were obtained in units of millivolts and picoamperes, and the latter were converted to $\mu A/cm^2$ (for scaling the I–V curves) by estimating the diameter of each L cell with an ocular micrometer and converting to the surface area of a simple sphere. From the electron microscope study of Price (1970), surface filopodia on the L cell would increase the actual membrane surface by 2- to 3-fold, which would correspondingly reduce calculated membrane current densities and conductances.

RESULTS

Whole-cell recording. Progressive sealing between each patch electrode and the cell membrane was monitored with bipolar current pulses through the patch amplifier (100 pA initially, less as sealing progressed). While the tip of the patch electrode was manoeuvred against the cell surface, slight positive pressure was applied to the capillary fluid; sudden release of that pressure usually then resulted in formation of a 10–20 MΩ contact. If a gigohm (GΩ) seal did not develop spontaneously within the next 2–3 min, gentle suction was exerted, which usually increased the resistance to 100–500 MΩ. Thereafter the seal either stabilized (preparation discarded), or increased

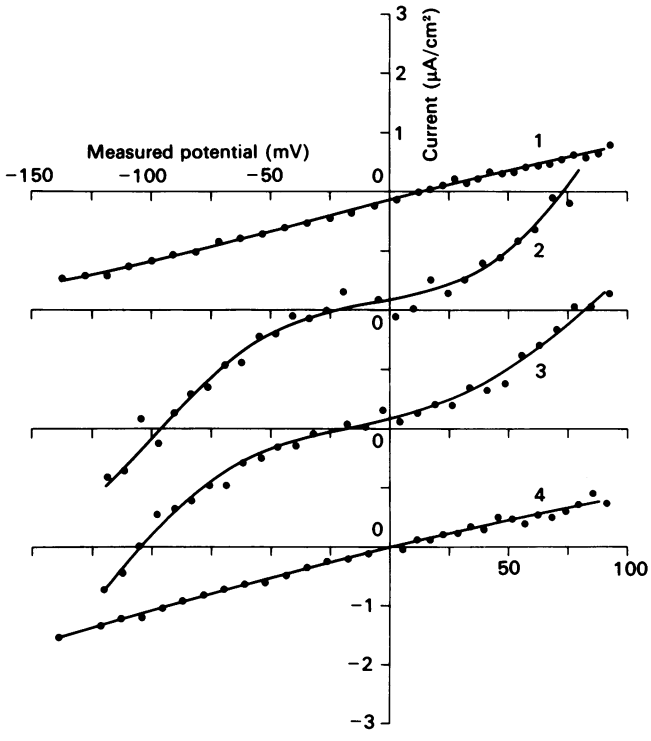

Fig. 3. Demonstration of current–voltage (I–V) measurement, and procedures for analysis. Membrane properties with low 'intracellular' free Ca^{2+}. 1, I–V scan with 19 GΩ seal, and patch membrane still intact. Plotted points represent the paired values of measured current and voltage. Note that after the seal had formed, the pipette interior was slightly (11 mV) positive to zero, with no injected current. Smooth curve is a least-squares polynominal through the points. 2, I–V scan 0·15 min after membrane patch was ruptured by sharp suction. Again, points show the actual I–V data and smooth curve is a least-squares polynominal. The potential for zero current is now negative, about −22 mV. 3, similar to 2, but 1·3 min after rupture. 4, 2·9 min after patch rupture and 0·4 min after patch had resealed. Polynomial coefficients for the smooth curves drawn:

Curve no.	a_0 ($\times 10^{-1}$)	a_1 ($\times 10^{-3}$)	a_2 ($\times 10^{-5}$)	a_3 ($\times 10^{-7}$)	a_4 ($\times 10^{-9}$)	a_5 ($\times 10^{-11}$)
1	−1·396	10·54	−0·5129	−0·6874	0	
2	1·772	7·360	5·323	29·07	1·409	−6·887
3	1·606	9·960	8·667	16·89	−6·051	−4·862
4	−0·0499	9·751	−0·8374	0		

Cell bathing medium, SBM: 160 mM-NaCl, 6 mM-KCl, 2 mM-$CaCl_2$, 1 mM-$MgCl_2$, 0·25 mM-K_2HPO_4, 10 mM-HEPES–NaOH (pH 7·3). Pipette solution: 150 mM-KCl, 1 mM-$MgCl_2$, Ca EGTA (10^{-8} M-free Ca^{2+}), 10 mM-HEPES–NaOH (pH 7·3). Cell diameter, 13 μm; surface area (assumed smooth-sphere geometry), 530 μm^2; therefore the current calibration is 5·3 pA/cell = 1 $\mu A/cm^2$.

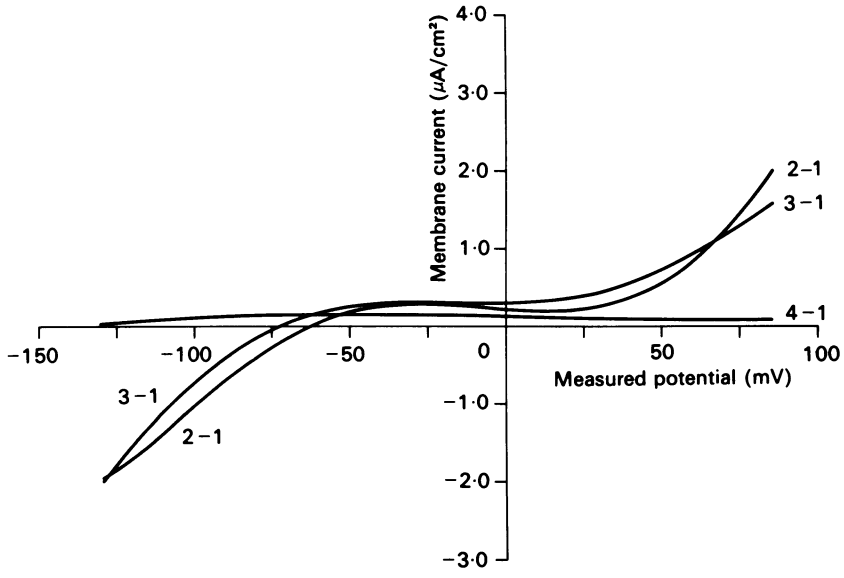

Fig. 4. Membrane I–V relationships, calculated as the difference I–V curves at 0·15 and 1·3 min after patch rupture (plus reseal control at 2·9 min). Data from Fig. 3, with fitted curve 1 subtracted from fitted curves 2 and 3 (and 4) in order to correct for current flow through the electrode seal. Corrected estimates of the resting (zero-current) membrane potential in this L cell are −67 mV (curve 2−1) and −77 mV (curve 3−1), with corresponding slope conductances of 19 and 17 μS/cm². Curves 2−1 and 3−1 are characteristic for membranes of cells studied with low intracellular free Ca^{2+}.

to the GΩ range (10–50 GΩ) within 20–45 s. Normally the membrane patch thus sealed on would persist without rupture for an hour or more, even with 2 mM-EGTA (free Ca^{2+} < 1 nM) in the electrode.

After control I–V measurements had been made via the standard voltage-clamp sequence, resistance monitoring with 0·1 pA current pulses was resumed, and a strong suction pulse was applied to the patch pipette. This sometimes had no effect (preparation discarded), but more often caused either rupture of the seal (collapse of resistance; preparation discarded) or rupture of the membrane patch, indicated by a rapid shift of the recorded voltage with an equally rapid, but small, decrease of resistance. Confirmation that this latter event initiated whole-cell recording came from several observations: (i) input capacitance was increased, as shown in Fig. 5, to the range of 10–20 pF, (ii) upon subsequent voltage-clamping, current noise was found to have increased appreciably, to nearly ±1 pA (low-pass cut-off at 500 Hz; see Figs. 3 and 5B), (iii) the input I–V relationship changed, becoming much steeper at voltages outside the range ±50 mV, as shown in Fig. 3 (compare curves 2 and 3 with curve 1), and finally, (iv) applied current pulses produced the h.a. described by Nelson *et al.* (1972), when free Ca^{2+} in the patch pipette was less than 1 μM (see Fig. 6, below). The success rate for patch-breaking was about 20%. Spontaneous closure of the pipette tip (presumed resealing of the patch, see curve 4 in Fig. 3) followed within 10 min in some cases, but re-entry could usually be achieved by repeated strong suction.

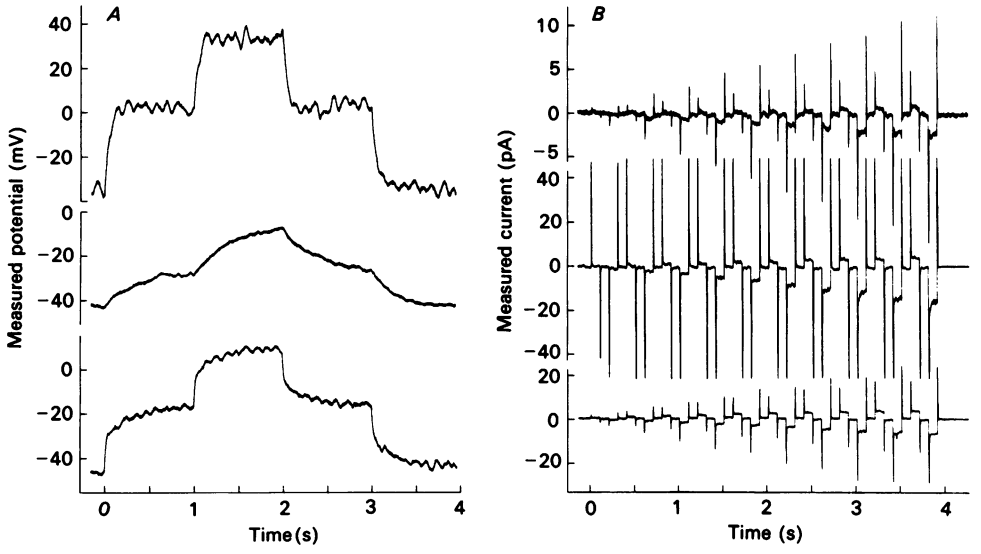

Fig. 5. *A*, voltage responses of a single cell when fixed-current pulses were applied in different recording modes. Top trace: cell-attached mode with pipette and stray capacitances compensated, ±0·5 pA pulses. Middle trace: whole-cell mode after applying a pulse of strong suction, ±1 pA. Bottom trace; outside-out patch obtained by drawing the pipette away from the cell, ±1 pA. The increase of input capacitance (middle trace) confirms the transition to whole-cell recording. The membrane capacitance can be estimated at ~ 15 pF, from the time constant (400 ms) and resistance (25 GΩ) evident in the middle trace, corrected by about 1 pF for the electrode capacitance. 15 pF implies a specific membrane capacitance of ~ 2·2 μF/cm^2, uncorrected for surface filopodia (Price, 1970). The noise at 8–9 Hz is microphonic. *B*, current traces during *I–V* scans (range −125 mV to 50 mV) recorded after the corresponding traces in *A*. Note that charging currents were greatly increased in the whole-cell mode. In this case input resistance during whole-cell recording was reduced to 30–40 % of that during cell-attached recording, but was approximately equal to that subsequently seen with the outside-out patch. Standard pipette solution and SBM were used, as in Fig. 3.

Patch and seal resistances. Validation of the *I–V* subtraction procedure requires demonstrating both that the small-patch resistance (during cell-attached recording) is large compared with the seal resistance and that the seal resistance itself is constant during rupture of the membrane patch. Fenwick *et al.* (1982), working with excitable (chromaffin) cells, reported that spontaneous pipette currents, ranging from 0·2 pA to several picoamperes, flowed into the cytoplasm, when pipettes were held at bath potential and pipette solution was identical to the bath solution. They also observed associated spontaneous excitation, and concluded that the patch resistance could be the same order of magnitude as the seal resistance. In cell-attached recordings of L cells, however, offset currents always were smaller than 0·2 pA in usable preparations, and usually were hyperpolarizing to the whole-cell membrane (e.g. see Fig. 3, curve 1). Such data do not implicate a leaky patch. (Exceptions to the above statements did occur, under the specific condition that an appreciable bag of cytoplasm could be seen (with phase contrast optics, 200 ×), as happened with larger diameter pipettes or when prolonged suction was required to initiate the gigohm seal.)

Absolute constancy of the seal resistance, during patch rupture, cannot be guaranteed, but several observations militate against serious errors from this source. It should first be noted that for the over-all conclusions to be drawn from the L-cell experiments, only *increases* of seal resistance, at or following patch rupture, are deleterious. Once gigohm seals had formed we never observed resistance increases which could be attributed to seal behaviour. This was true whether the primary membrane patches (cell-attached recording) were held for 30 min or longer, whether broken patches resealed, whether whole-cell recording was sustained for long periods, or whether the patch electrode was drawn away from a whole cell to form an outside-out patch. In the majority of cases the transition from cell-attached recording to whole-cell recording was accompanied by no change or a slight decrease of input resistance over the voltage range −40 to +25 mV, as illustrated in Fig. 3. In some cases a 2–3-fold decrease of input resistance occurred, as in Fig. 5 (cf. top and middle records), but then subsequent formation of outside-out patches took place with little or no resistance change (Fig. 5, cf. middle and bottom records). The simplest interpretation of these observations is that seal resistance tends to decrease, not increase, during transitions between different recording modes, and that in the range −40 to +25 mV the whole-cell membrane resistance is larger than the seal resistance. (Mechanical stability of the seals was further attested by the fact that, after patch rupturing, L cells could be moved about in the chamber attached only to the patch electrode, with no significant change of input resistance over periods of 10–30 min (again, see Fig. 3).)

Resting membrane potential and I–V relationships with low Ca^{2+} concentrations. As was shown in Fig. 3, when free Ca^{2+} in the patch pipette was kept below 1 μM, patch rupture changed the shape of the recorded (input) *I–V* curve, but with little effect on the mid-range slope conductivity. The open-circuit voltage (zero applied current) shifted from a few millivolts positive to the range of −10 to −25 mV, which corresponds to the resting membrane potential usually reported from L cells. Subtraction of the pre-rupture *I–V* curve yields estimated membrane *I–V* curves of the shape shown in Fig. 4 (curves 2−1, 3−1), having nearly zero conductance in the voltage range −40 mV to +25 mV, membrane potentials of −50 to −75 mV (average −64·7 ± 3·2 mV, mean ± S.E. of mean for nine cells), and slope conductivities near 50 μS/cm² at high membrane potentials (negative or positive). The over-all curve shape, at least for membrane potentials negative to +30 mV, strongly resembles anomalous rectification, as described in striated muscle, egg cells etc. (Katz, 1949; Hagiwara & Takahashi, 1974; Adrian, 1969). The resting values of both membrane potential and membrane conductance were independent of extracellular Ca^{2+} in the range 2–8 mM, and independent of intracellular free Ca^{2+} over the range 1–500 nM.

Recordings with conventional penetrating micro-electrodes, in irradiated or confluently grown giant L cells, frequently display fluctuations of potential between the values (*ca.* −15 mV and −50 to −60 mV) thought to represent spontaneous activation of Ca^{2+}-sensitive K^+ channels (Okada *et al.* 1977, 1979; Roy & Sauve, 1983). No such fluctuations were observed in the present patch-electrode experiments, as long as free Ca^{2+} in the electrode was kept below 1 μM. However, as is shown in Fig. 6, brief pulses of inward current (hyperpolarizing, typically 250 pA for 0·5 s) could trigger voltage swings of 30–60 s duration which appeared identical to the h.a.

(triggered opening of the Ca^{2+}-dependent K^+ channels) carefully described in giant L cells (Nelson *et al.* 1972; Okada *et al.* 1979; Okada, Tsuchiya & Yada, 1982). The membrane *I–V* curves obtained before h.a. in the experiment of Fig. 6 (0·15 min after patch rupture) and during the second hyperpolarizing swing (2·8 min) are displayed in Fig. 7. Fig. 7*A* shows the curves on an expanded current scale, appropriate for normal L cells; Fig. 7*B* shows the curves on a scale appropriate for h.a. The

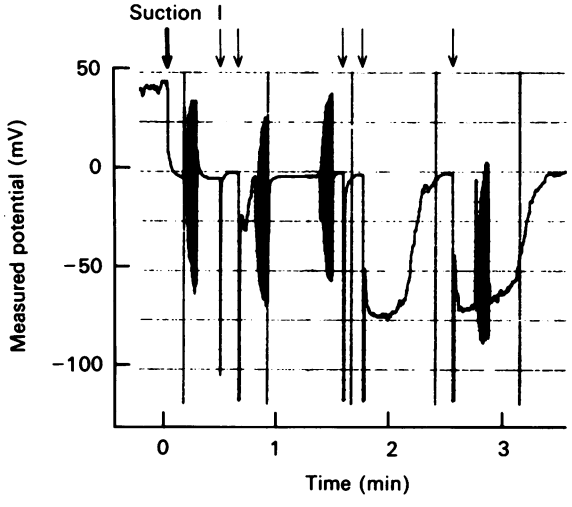

Fig. 6. A chart recorder tracing of voltage at the patch electrode, for an electrode containing $< 10^{-9}$ M-free Ca^{2+}, to illustrate the induction of 'hyperpolarizing activation' (h.a.; Nelson *et al.* 1972) by strong current pulses. Dark arrow: suction to break the membrane patch; black wedges on the record: attenuated signals from voltage-clamp scans for *I–V* curves; light arrows: inward current pulses, 250 pA × 0·5 s; only the last two (out of five) pulses elicited the h.a. response. Cell bathing medium: 160 mM-NaCl, 6 mM-KCl, 8 mM-$CaCl_2$, 1 mM-$MgCl_2$, 0·10 mM-K_2HPO_4, 10 mM-HEPES–NaOH (pH 7·3). Pipette solution: 150 mM-KCl, 1 mM-$MgCl_2$, 2 mM-EGTA, 10 mM-HEPES–NaOH (pH 7·2).

h.a.-associated increase in slope conductance, for example at −50 mV, was 53-fold: from 7·2 to 380 μS/cm^2. This is a (10-fold) larger proportionate change in conductance than has generally been reported in h.a., partly because leakage through the seal (6·2 μS/cm^2) was subtracted. It also is associated only with a small increase of membrane potential, (−)21 mV, compared with (−)40–60 mV usually reported (Okada *et al.* 1979; Nelson *et al.* 1972).

Over-all membrane behaviour with elevated intracellular Ca^{2+} concentrations. Under initial conditions (1–3 min after patch rupture) with free Ca^{2+} greater than 100 μM in the patch-electrode solution, the resting membrane potential (Fig. 8) and *I–V* curve (Fig. 9, upper trace) closely resembled those observed during pulse-triggered h.a. Inspection of the voltage traces, however, reveals a clear two-step change in recorded voltage as the patch ruptured: first (1–5 s) to the neighbourhood of −10 mV, and then to about −70 mV. It is reasonable to suppose that the first step corresponds to the recorded (uncorrected) potential with < 1 μM-free Ca^{2+}, while the second ensues from Ca^{2+} leakage and represents opening of the Ca^{2+}-sensitive K^+ channels

(Okada *et al.* 1982; also see above). Further evolution of the membrane *I–V* relationship occurred over a period of 15 min or more. Fig. 9, which gives a sample of *I–V* curves taken at several different times along the voltage tracing of Fig. 8, demonstrates a progressive decline of slope conductance (*ca.* 10-fold, at the voltage intercept) and membrane potential (by *ca.* 25 mV) lasting for about 6 min (Fig. 9*A*).

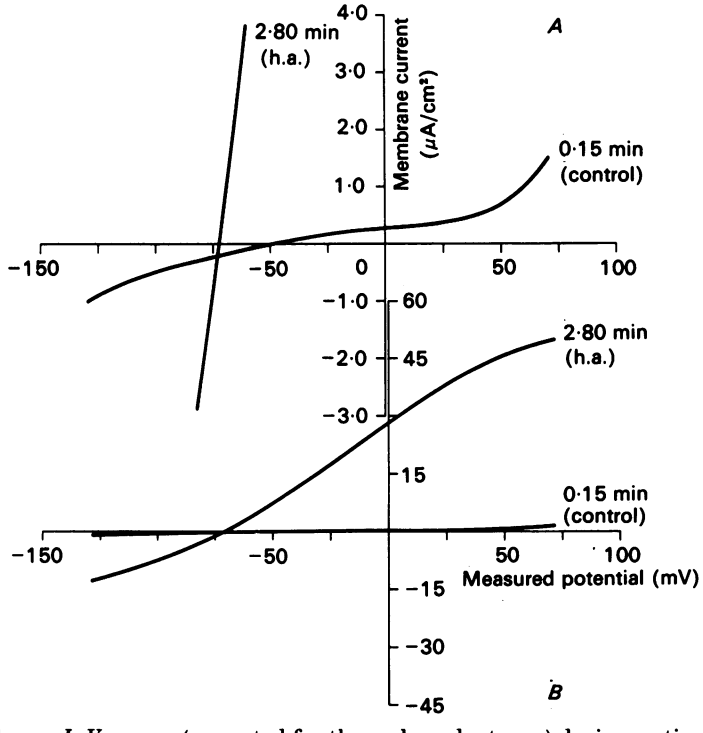

Fig. 7. Membrane *I–V* curves (corrected for the seal conductance) during resting and h.a. states. Curves from the data in Fig. 6. *A*, ordinate scale (current) appropriate for resting membrane. *B*, same results as in *A*, but with ordinate scale appropriate for h.a. state of membrane. A control (leakage) *I–V* curve was taken before membrane patch was ruptured. Note relatively small change in the zero-current potential: from −54 to −76 mV during h.a.; but the large change of slope conductance: from 8 to 316 μS/cm^2.

Beyond that time membrane potential appeared to oscillate slowly, with repolarization (7–10 min, Fig. 9*B*) accompanied by increasing membrane conductance, and subsequent depolarization accompanied by decreasing conductance. Qualitatively, this behaviour would be consistent with oscillation of the mean number of Ca^{2+}-switched channels open, but quantitatively the *I–V* curves suggest changes also of specificity, either in the background conductance of the membrane or in the Ca^{2+}-dependent channels themselves (see especially the depolarization, with little conductance change, between 15·1 and 16·75 min).

Short-term stability of the Ca^{2+}-dependent conductance. Close examination of the usual *I–V* records obtained with pipette/cytoplasm Ca^{2+} concentrations greater than 0·1 mM revealed a tendency for the measured current to increase with time during

reverse polarization of the membrane. Since such an effect could in principle falsify the *I–V* curves in Fig. 9, a more careful study of the current wave forms was undertaken. In particular, *I–V* curves were generated with a small number (ten) of voltage pulses of long duration (400 ms). The results of a typical experiment of this sort are shown in Fig. 10*A*, using the customary repetitive display. It is evident that,

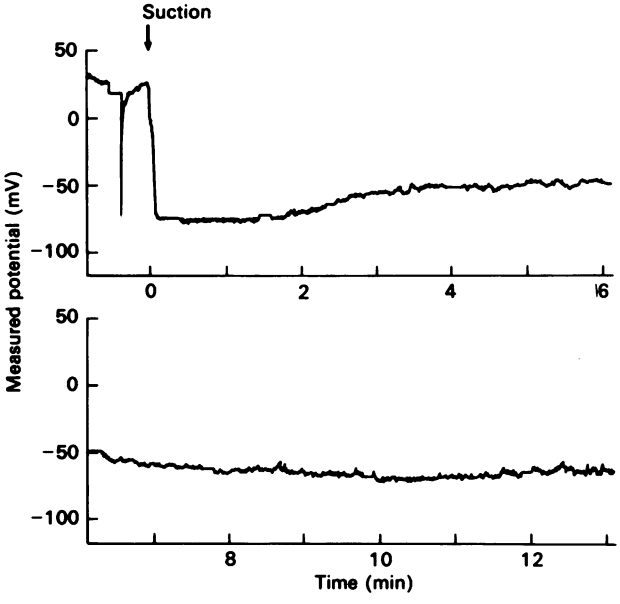

Fig. 8. Tracing of voltage record from a cell with the patch pipette containing high (1 mM) free Ca^{2+}. Lower trace continued from upper one. Voltage-clamp pulses (similar to those in Fig. 6) have been removed for clarity, but their positions are designated by the 10 s 'flats' in the tracing. Note the two-stage shift of measured voltage when suction was applied to rupture the membrane patch; also the slow oscillation of potential over the 14 min interval shown. Cell bathing medium as in Fig. 3. Pipette solution: 150 mM-KCl, 1 mM-$MgCl_2$, 1 mM-$CaCl_2$, 10 mM-HEPES–NaOH (pH 7·2).

for the large depolarizing steps, 'steady-state' clamp current is perhaps 10 % smaller initially than after several hundred milliseconds. *I–V* curves extracted from these data at two times, 90 ms (□) and 390 ms (●), are shown in Fig. 10*B*, along with one obtained from a single 3·0 s linear voltage ramp. None of the plots differs significantly from that obtained at 100 ms, corresponding to the data in the previous Figures.

Ionic specificity in the Ca^{2+}-dependent conductance. It seemed likely, from the magnitude of the normal resting membrane potential in L cells and from the previous published information on h.a., that conductance of the L-cell membrane under both conditions should be dominated by K^+. Direct confirmation of this idea was obtained by substitution of SBM (6·5 mM-K^+) by media containing 5, 20, 35 or 150 mM-K^+. Fig. 11 shows *I–V* curves for one case, in which $[K^+]_o$ was shifted from 6·5 mM (curve 1) to 150 mM (curve 2) and then back to 6·5 mM (curve 3). The shift in voltage intercepts (corrected for leakage through the electrode seal) is obvious. Data for this

and two more experiments are plotted in the inset to Fig. 11, where the line drawn gives the Nernst potential for K^+, in the patch electrode solution *vs.* the bathing medium. The observed least-squares slope for all the voltage data was 50 mV/10-fold concentration change, rather than 59 mV.

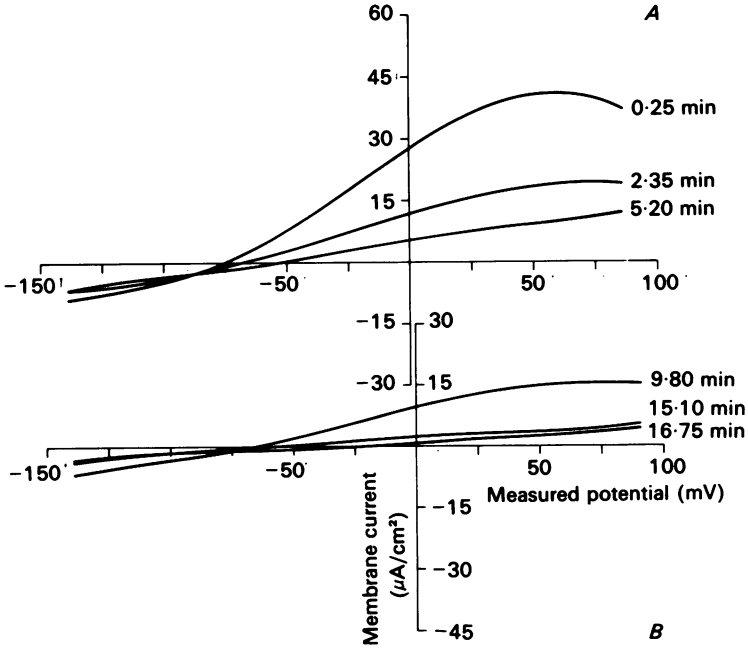

Fig. 9. Membrane *I–V* curves with the patch pipette containing 1 mM-free Ca^{2+}. Data from the experiment of Fig. 8, with *I–V* curves taken at the times indicated. Correction for the pipette seal was negligible with high Ca^{2+} in the pipette. *A*, curves selected during the first depolarizing swing in Fig. 8. *B*, curves selected during subsequent hyperpolarization and the second depolarization (time beyond 14 min, not shown in Fig. 8). Note that substantial depolarization occurred in the second case with little change in membrane conductance (cf. curves at 15·1 and 16·75 min).

Corresponding data obtained with patch electrodes containing 1 mM-Ca^{2+} are shown in Fig. 12. In these experiments the membrane potential was allowed to stabilize (i.e. to the condition at about 6 min in Fig. 8) before $[K^+]_0$ was shifted, so that only a fraction of the total number of Ca^{2+}-activatable channels were open. (It is nevertheless clear from the shapes of the *I–V* curves and the scale on the current axis in Fig. 12, compared with Fig. 11, that Ca^{2+}-activated permeability was dominant.) The reversible shift in voltage intercept with changed $[K^+]_0$ was again clear, and the slope of membrane potential *vs.* $[K^+]_0$ closely approximated the Nernst slope (Fig. 12, inset).

Okada *et al.* (1979) reported that injection of Sr^{2+}, Mn^{2+}, or La^{3+} into giant L cells could also activate Ca^{2+}-dependent K^+ conductance, but Mg^{2+} and Ba^{2+} could not. In the present experiments, 1 mM-Sr^{2+} mimicked 0·1–1·0 mM-Ca^{2+} very closely (records not shown), whereas the 1 mM-Mg^{2+} normally present in patch-electrode solution did not activate at all.

Co^{2+} (1 mM) and Ba^{2+} (5 mM), on the other hand, had a surprising and quite different effect. Voltage records from two L cells sealed to electrodes containing either 1 mM-Co^{2+} or 5 mM-Ba^{2+} are shown in Fig. 13. For both cations, the potential measured immediately after patch rupture (uncorrected for leakage through the pipette seal) was characteristic of cells studied with < 1 μM-Ca^{2+}. However, after a

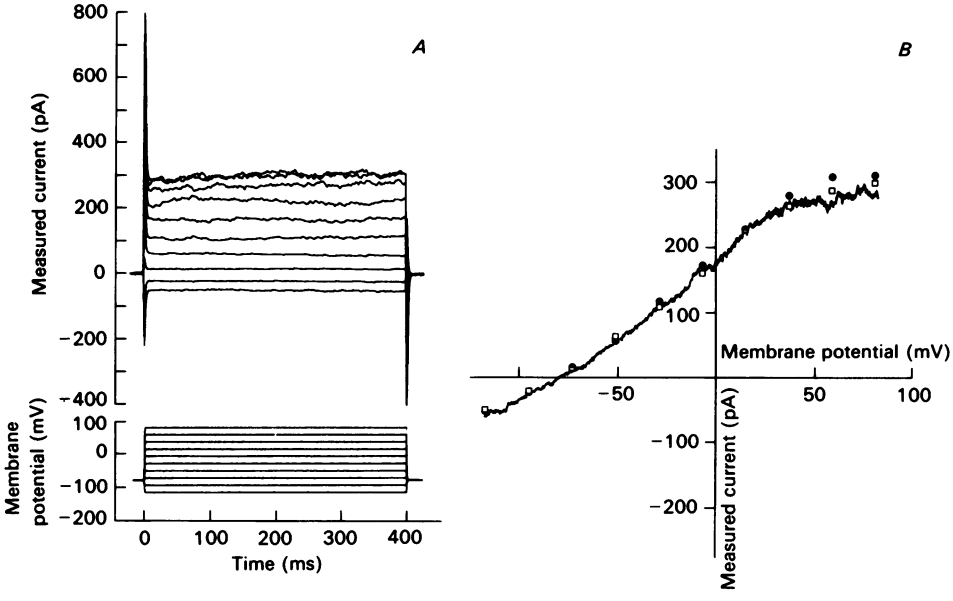

Fig. 10. Short-term stability of membrane I–V data in the Ca^{2+}-activated state. *A*, repetitive display of clamping currents (upper records) required to create voltage pulses between −120 mV and +80 mV (lower records), during whole-cell recording. With reverse polarization, required current is smallest immediately after the capacitative transient and is maximal at about 200 ms. *B*, I–V plots of the data in *A*, compared with an I–V ramp lasting 3·0 s. □, currents averaged over the interval 90–100 ms; ●, currents averaged over the interval 390–400 ms; trace, current record during the voltage ramp. Standard bathing medium; pipette solution contained 1 mM-$CaCl_2$, as in Fig. 8.

variable interval (0·5–10 min) sudden hyperpolarization occurred, to give measured potentials of about −60 mV. Then after another variable period (1–3 min), the membrane depolarized again, with each full cycle resembling the familiar hyperpolarizing activation. Superficially, these results might suggest that, contrary to the findings of Okada *et al.* (1979), Co^{2+} and Ba^{2+} can activate the Ca^{2+}-dependent K^+ channels, but with on- and off-time courses very different from those seen with Ca^{2+}. However, I–V analysis belies this simple interpretation. Comparison of the I–V plots in Fig. 14 (*A*: Co^{2+}; *B*: Ba^{2+}) with those in Fig. 9 shows two major differences: (i) a region of apparent negative membrane conductance, which is only hinted by the Ca^{2+} curves at strong positive membrane potentials, is well defined with both Co^{2+} (+25 to +75 mV) and Ba^{2+} (−25 to +25 mV) in the 'channel-open' state, which may indicate that Co^{2+} and Ba^{2+} may exert a voltage-dependent block more strongly than Ca^{2+} does at high concentrations (Marty, 1981; Vergara & Latorre, 1983); and (ii)

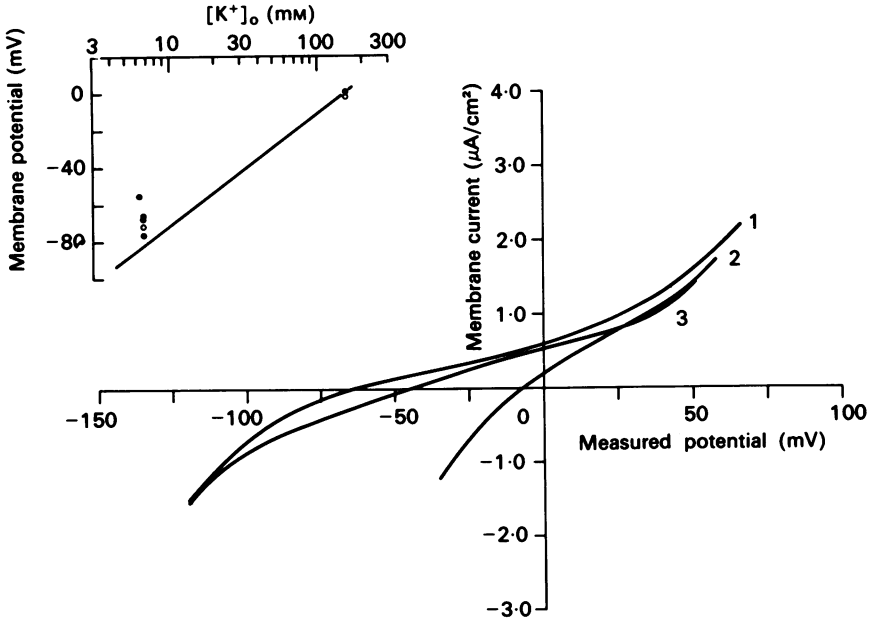

Fig. 11. K^+ sensitivity of the (corrected) membrane potential, in the resting state (low internal Ca^{2+}). Cell bathing media: for low $[K^+]$, same composition as in Fig. 3; for high $[K^+]$, 150 mM-KCl, 1 mM-$CaCl_2$, 1 mM-$MgCl_2$, 10 mM-HEPES–NaOH (pH 7·3). Pipette solution: 75 mM-K_2SO_4, 1 mM-$MgCl_2$, Ca EGTA (free $Ca^{2+} = 10^{-8}$ M), 10 mM-HEPES–NaOH (pH 7·2). The following table lists key parameters from the *I–V* curves drawn:

Curve no.	Time after patch rupture (min)	$[K^+]_o$ (mM)	Membrane potential (mV)	Slope conductance at zero current (μS/cm²)
1	3·7	6·5	−73·6	12·5
2	4·9	150	−2·8	32·1
3	5·6	6·5	−54·3	13·6

Inset: summary plot of membrane potential *vs.* $\log[K^+]_o$, for three experiments in which changes of bathing solution were successful. All values were corrected by adding the liquid junction potentials (see Fig. 2) to the zero-current voltages from membrane *I–V* curves. The total junction potential with K_2SO_4 solution in the patch pipette was 10·3 mV when $[K^+]_o$ = 6·5 mM, and was 5·8 mV when $[K^+]_o$ = 150 mM. The continuous line indicates the Nernst relationship. Plotted data points were obtained from this Figure (○) and from two other experiments (with Cl^- in the pipette; ●). For the reference condition, with $[K^+]_o$ = 6·5 mM, the membrane potential averaged −64·7 ± 3·2 mV (S.E. of mean for nine cells).

the subsequent depolarization (*I–V* curves at 6·1 min for Co^{2+} and 2·15 min for Ba^{2+}) occurs with *membrane conductance still high*. The simplest interpretation of these findings is that Co^{2+} and Ba^{2+} are indeed able to open the Ca^{2+}-dependent K^+ channel, but also alter its ion specificity. The two effects certainly do occur on peculiar time scales: delayed with respect to normal Ca^{2+} activation, and faster than the spontaneous closure seen with sustained Ca^{2+} (Fig. 9*B*).

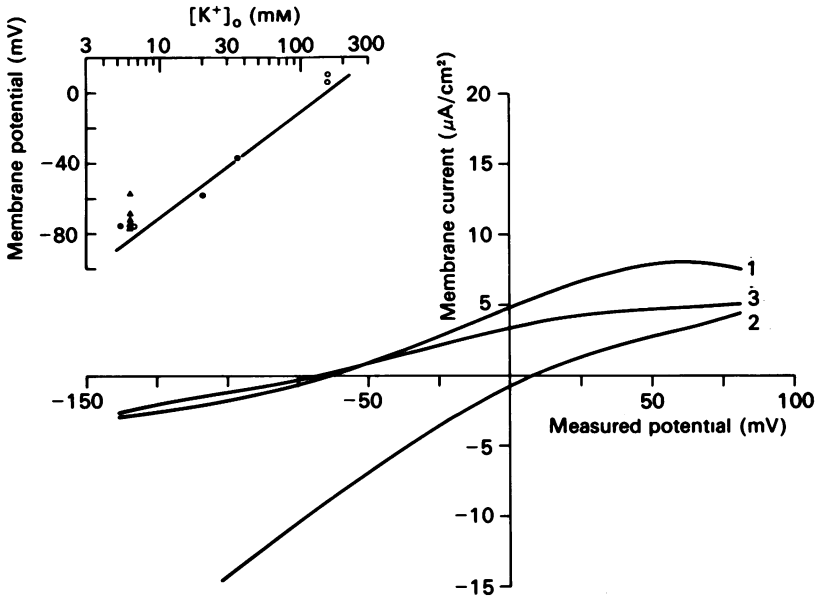

Fig. 12. K^+ sensitivity of the (corrected) membrane potential, in the Ca^{2+}-activated state. Cell bathing media: as in Fig. 11. Pipette solution: 75 mM-K_2SO_4, 1 mM-$MgCl_2$, 1 mM-$CaCl_2$, 10 mM-HEPES–NaOH (pH 7·2). Table of parameters from the *I–V* curves drawn:

Curve no.	Time after patch rupture (min)	$[K^+]_o$ (mM)	Membrane potential (mV)	Slope conductance at zero current (μS/cm²)
1	4·3	6·5	−75·3	61·4
2	5·4	150	+4·2	93·0
3	7·9	6·5	−77·3	46·4

Inset: summary plot of membrane potential *vs.* $\log[K^+]_o$, for four experiments in which changes of bathing solution were successful. All values corrected for liquid junction potentials as in Fig. 11. Continuous line indicates the Nernst relationship. Plotted data points were obtained from this Figure (○) and from two other experiments (with Cl^- in the pipette); one with activation by 1 mM-Sr^{2+} (●) and the other from Fig. 8 (△). For the reference condition, with $[K^+]_o = 6·5$ mM, the membrane potential averaged $-74·1 \pm 2·0$ mV (S.E. of mean for ten cells).

DISCUSSION

Re-evaluation of voltage-measuring techniques. Lamb & MacKinnon began their 1971 exposition of the electrophysiological properties of cultured fibroblasts with the following simple and clear synopsis of information at that time: 'Cells which are electrically excitable are characterized by having a high membrane potential at rest, whereas many small inexcitable cells have low membrane potentials.' They went on to explore several likely physiological interpretations of these facts, and concluded, finally, that 'the low membrane potential of these cells arises because of a low absolute P_K', with the Na^+:K^+ permeability ratio (P_{Na}/P_K) being 0·67. The interpretation fits nicely with a general bias that Cl^- should be passively distributed; in the case of L

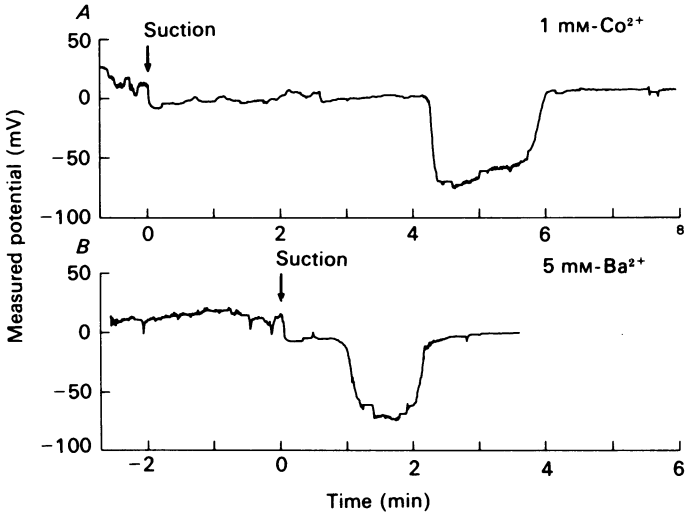

Fig. 13. Effects of Co^{2+} and Ba^{2+} on potential recorded by whole-cell patch electrode. Patches were broken by sharp suction at the heavy arrows. Note long delay before the abrupt negative shift, and then rapid return of voltage after 1–2 min (cf. Fig. 8). Cell bathing medium as in Fig. 8. Pipette solutions as in Fig. 8, but with the 1 mM-$CaCl_2$ substituted by 1 mM-$CoCl_2$ (*A*) or 5 mM-$BaCl_2$ (*B*). Positions of *I–V* scans indicated by 'flats' on the tracing of voltage.

cells, $[Cl^-]_i/[Cl^-]_o = 70$ mM/147 mM, giving an E_{Cl} of -19 mV compared with measured membrane potentials of -15 mV.

It has, in fact, become generally accepted that the physiological resting membrane potentials of isolated small mammalian cells are low, despite several disconcerting facts: (i) measurements made with distribution indicators have given large membrane potentials under conditions where electrodes give small values (see, e.g., Laris, Pershadsingh & Johnstone, 1976; Johnstone, 1978); (ii) numerous warnings have been issued about leakage and other artifacts associated with conventional microelectrode techniques (see Introduction); (iii) the curious observation that the Na^+:K^+ mobility ratio in free solution is 0·67 (Hodgkin, 1958), like the permeability ratio mentioned above, so the L-cell membrane would appear to be non-selective with respect to cations (see also Roy & Okada, 1978); and (iv) an indirect conclusion that the conductivity of some cell membranes (e.g. red blood cells) is very low indeed (1 μS/cm^2 or less (Lassen, 1977)), so that cell input resistances of 10 GΩ or greater could be expected.

The latter two facts in particular suggest that the low values of membrane potential reported in many different cultured cells could result from short-circuiting of the actual membrane potential by leakage through the membrane-to-glass seal. With respect to this kind of artifact, patch electrodes offer a potential major advantage (over conventional penetrating electrodes): in addition to the tighter seals which they can form, they permit direct assessment of the seal characteristics. In the present experiments with L cells, the absolute resistance of the membrane within patch pipettes was expected to be well above the seal resistance (see discussion of Fig. 5),

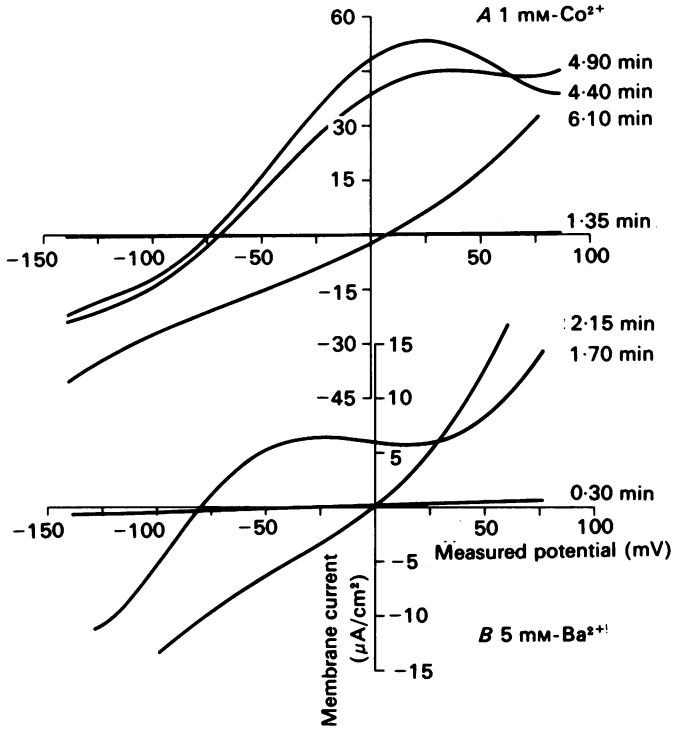

Fig. 14. Membrane *I–V* curves showing effects of Co^{2+} and Ba^{2+}. From experiment of Fig. 13. Note that slope conductance at the zero-current potential is about 3-fold smaller in Ba^{2+} than in Co^{2+} (see change of ordinate scale between *A* and *B*), and that the negative-slope region is shifted leftward (1·7 min Ba^{2+} curve *vs.* 4·4 min Co^{2+} curve). In both cases the final depolarization occurred with the membrane still in a high-conductance state (2·15 min Ba^{2+} curve, 6·1 min Co^{2+} curve).

and *I–V* scans taken after seals had formed but before the membrane patches had broken (e.g. Fig. 3, curve 1), described the seals. Slope conductances of 20–100 pS (resistances of 10–50 GΩ) were observed with zero-current voltages of −5 to +40 mV. Small offset potentials at zero-current clamp were difficult to eliminate with input resistances well over 10 GΩ, because of clamping circuit inaccuracy in the range of 0·1 pA. Furthermore, the observed offsets may have reflected variable selectivity of the seal (pipette solutions contain ~ 150 mM-K^+; cell bathing solutions, ~ 150 mM-NaCl). Subtraction of seal *I–V* curves from the corresponding whole-cell curves should yield the 'true' membrane *I–V* characteristics, as for example in Figs. 4 and 7. Thus, resting membrane potentials of −50 to −75 mV were obtained under conditions in which previous studies have reported −15 to −20 mV. Such findings make clear that all earlier reports of low resting membrane potentials, and resistivities in small cultured cells must be re-examined.

Although uncontrolled *increases* of seal resistance during rupture of the membrane patch could falsify these corrected membrane potentials on the *high side*, we have argued that such does not occur under our recording conditions with L cells (see

discussion of Fig. 5). Uncontrolled *decreases* of seal resistance would falsify voltage measurements on the *low side*, so artifacts in that direction cannot account for quantitative discrepancies between these and previous experiments. Large decreases of sealing resistance, of course, were easily spotted (especially with low Ca^{2+} in the patch electrode), and such cells were discarded.

However, it must be admitted that uncontrolled, but small, decreases of sealing resistance at the time of patch rupture could contribute to the scatter in values of resting membrane potential, and to the rather large range of observed values; in that case, the largest values (*ca.* −75 mV) would be best estimates of the true resting membrane potential in L cells. As a general practice, it may be most satisfactory to estimate seal resistances from the quiescent leakage with outside-out patches, or (for L cells) from the mid-range linear portion of whole-cell *I–V* curves.

I–V relationships and membrane selectivity. Perhaps the most remarkable information to emerge from these measurements is the shape of the *I–V* relationship for the resting L-cell membrane, and the conductance scale. As shown in Figs. 4 and 7, and compressed in Fig. 14 (times 1·35 min and 0·30 min), the membrane *I–V* curve with low $[Ca^{2+}]_i$ is distinctly flat in the mid range of potentials, having a slope conductance $\simeq 0$, or slightly negative. Even at the zero-current potential, slope conductivity is low, between 5 and 15 $\mu S/cm^2$ in different experiments, calculated from smooth-sphere geometry. That would be reduced still 2–3-fold by including the surface of filopodia (Price, 1970), so resting resistivities well above 100 $k\Omega \cdot cm^2$ characterize the L-cell membrane, compared with values of 10–20 $k\Omega \cdot cm^2$ reported previously (Nelson *et al.* 1972; Okada *et al.* 1977). The strong non-linearity of the corrected *I–V* curves for L-cell membranes can be taken as evidence that current leakage at the membrane-to-glass seals has been correctly compensated, since appreciable leakage would impose a linear component on the over-all *I–V* curve. However, the physical basis for the observed non-linearity is uncertain. At potentials negative to +25 mV, the curves resemble an anomalous rectifier and perhaps should be examined further in relation to the 'residual' anomalous rectifier or time-independent 'background' rectifier familiar from excitable membranes (Noble & Tsien, 1968; Noble, 1962; Cleemann, 1981; Hume & Giles, 1983). However, at potentials positive to +25 mV, conductance again increases, so the over-all *I–V* curve resembles those predicted by a variety of channel models and mobile site models functioning without rate limitation in scalar chemical reaction steps (Adrian, 1969).

In the absence of a quantitative theory to describe the *I–V* relationship for the resting L-cell membrane, rigorous assessment of membrane selectivity is really not possible. However, some simple considerations can yield estimates of relative permeabilities. With SBM outside the cells, and standard pipette solution in the patch pipette, diffusion potentials for the major ions are: $E_K = -80$ mV, $E_{Na} = +77$ mV, and $E_{Cl} = -3$ mV; with K_2SO_4 in the pipette solution, E_{Cl} changes to −109 mV. Now, since the presence of low or high Cl^- in the patch pipette (i.e. sulphate-substituted or not) has no effect on the zero-current potential (Fig. 11, inset) or shape of the *I–V* relationship (Figs. 4, 7 and 11), we conclude that G_{Cl} is negligible. This result contrasts directly with the supposition of Lamb & MacKinnon (1971*a*, *b*), that the large isotopic Cl^- flux would be current-carrying, and argues that the major Cl^- transport process in L cells is electrically silent, like that in erythrocytes (Lassen, Pape

& Vestergaard-Bogind, 1978) in certain heart-muscle cells (Piwnica-Worms, Jacob, Horres & Lieberman, 1983), and in proximal tubular cells of the kidney (Shindo & Spring, 1981; Guggino, London, Boulpaep & Giebisch, 1983). With resting membrane potentials of -50 to -75 mV and the values of E_K and E_{Na} noted above, linear equivalent-circuit theory would yield conductance ratios (G_{Na}/G_K) of 0·033–0·24. If activity coefficients for the two ions are assumed equal, the constant-field theory (Hodgkin & Katz, 1949) yields permeability ratios (P_{Na}/P_K) of 0·0095–0·091. With a total membrane conductivity of 10 μS/cm^2, the specific ion conductivities would be G_{Na} = 0·3–1·9 and G_K = 8·1–9·7 μS/cm^2.

(Two points should be made about the earlier measurements of L-cell membrane potential and conductivity. Partly because of the pioneering nature of those studies, the authors were alert to possible artifacts (see, e.g., p. 323 of Okada *et al.* 1977) and opted to use irradiation-induced giant cells rather than ordinary L cells, in order to minimize the leakage problem. Since our present experiments have not explored the giant L cells, the possibility remains that normal suspension-cultured L cells and giant L cells do have different membrane properties. This is an important matter for further experiments.)

Ca^{2+}-dependent K^+ channels and h.a. The shift in membrane properties which accompanies either a sharp hyperpolarizing current pulse or deliberate introduction of Ca^{2+} to the electrode solution is completely consistent with the previous identifications of Ca^{2+}-dependent K^+ channels in L cells (Henkart & Nelson, 1979; Okada *et al.* 1979, 1982). In particular, the slope conductivities at the zero-current potential, 200–400 μS/cm^2, are similar to values which can be computed from previous data on giant L cells (Nelson *et al.* 1972; Roy & Okada, 1978). However, because of the decreased leak in present experiments, and the difference I–V method for compensating the leak, the increment of membrane potential produced by Ca^{2+} activation is now smaller than reported formerly. This is a simple consequence of the fact that in either the resting or the Ca^{2+}-activated state the L-cell membrane approximates a K^+ electrode (Figs. 11 and 12), so the effect of increasing absolute K^+ conductance tends to be voltage-clamping near E_K, rather than voltage-shifting toward E_K. The simple interpretation of large hyperpolarizations seen with penetrating electrodes and giant L cells is that the ~50-fold increase of membrane conductance with Ca^{2+}-activation diminished *relative* leak through the membrane-to-glass seal.

The slow shutting down of Ca^{2+}-activated K^+ current is similar, superficially at least, to the Ca^{2+}-dependent depression of Ca^{2+}-activated outward (K^+) current in snail neurones (Eckert & Lux, 1977). Both processes are probably derived from Ca^{2+} blockade of the Ca^{2+}-activated K^+ channels, which has been carefully described in cultured rat myotubes (by patch clamp: Methfessel & Boheim, 1982) and in rabbit skeletal muscle (bilayer reconstitution: Vergara & Latorre, 1983). The more complex and protracted consequences of Co^{2+} and Ba^{2+} treatment are consistent with generally complicated effects of Ba^{2+} on K^+ channels, but the present case could result from multiple actions of the two metal ions on the whole membrane, rather than from action on the K^+ channels alone.

Patch-clamp measurements on L-cell membranes have identified isolated Ca^{2+}-dependent K^+ channels which superficially resemble those reported in muscle (Pallota, Magleby & Barrett, 1981; Latorre, Vergara & Hidalgo, 1982), in chromaffin

and pituitary cells (Marty, 1981; Wong, Lecar & Adler, 1882), and in various nerve preparations (Adams, Constantin, Brown & Clark, 1982; Krueger, French, Blaustein & Worley, 1982). The large-conductance L-cell channels have open-state conductances of 200–300 pS (S. Hosoi & C. L. Slayman, unpublished observations), so the average density of the activated channels should be 1–5/100 μm^2, or 5–35/cell (for the normal suspension-cultured L cells). An effort is being made to compare these individual channels quantitatively with the whole membrane behaviour, after the manner of Lux & Brown (1984), particularly directed toward the origin of a membrane *I–V* relationship which saturates at strong negative *and* strong positive potentials (e.g. in Figs. 9*A*, 12 and 14).

The authors are indebted to Drs David Corey, Richard Aldrich and Gary Yellen for many helpful suggestions about the patch-clamp technique; to Dr E. A. Adelberg, Mr Jeremiah Donahue, and Ms Margaret Fairgrieve for advice and assistance with the L-cell cultures, and to Mr John Rose for computer programming and debugging. The work was supported by Research Grant PCM-7913412 from the National Science Foundation, and recently by Program Project Grant AM-17433 from the National Institute of Arthritis, Diabetes, and Digestive and Kidney Diseases.

REFERENCES

ADAMS, D. P., CONSTANTIN, A., BROWN, D. A. & CLARK, R. B. (1982). Intracellular Ca^{2+} activates a fast voltage-sensitive K^+ current in vertebrate sympathetic neurones. *Nature* **296**, 746–749.

ADRIAN, R. H. (1969). Rectification in muscle membrane. *Progress in Biophysics and Molecular Biology* **19**, 339–369.

BATES, G. W., GOLDSMITH, M. H. M. & GOLDSMITH, T. H. (1982). Separation of tonoplast and plasma membrane potential and resistance in cells of oat coleoptiles. *Journal of Membrane Biology* **66**, 15–23.

BLATT, M. R. & SLAYMAN, C. L. (1983). KCl leakage from microelectrodes and its impact on the membrane parameters of a nonexcitable cell. *Journal of Membrane Biology* **72**, 223–234.

BROWN, K. T. & FLAMING, D. G. (1977). New microelectrode techniques for intracellular work in small cells. *Neuroscience* **2**, 813–827.

CALDWELL, P. C. (1970). Calcium chelation and buffers. *Calcium and Cellular Function*, ed. CUTHBERT, A. W., pp. 10–16. London: Macmillan.

CLEEMAN, L. (1981). Heart muscle. Intracellular potassium and inward-going rectification. *Biophysical Journal* **36**, 303–310.

ECKERT, R. & LUX, H. D. (1977). Calcium-dependent depression of a late outward current in snail neurons. *Science* **197**, 472–475.

ETHERTON, B., KEIFER, D. W. & SPANSWICK, R. M. (1977). Comparison of three methods for measuring electrical resistances of plant cell membranes. *Plant Physiology* **60**, 684–688.

FELLE, H., STETSON, D. L., LONG, W. S. & SLAYMAN, C. L. (1979). Direct measurement of membrane potential and resistance in giant cells of *Escherichia coli*. *Frontiers of Biological Energetics*, vol. 2, ed. DUTTON, P. L., LEIGH, J. S. & SCARPA, A., pp. 1399–1407. New York: Academic Press.

FENWICK, E. M., MARTY, A. & NEHER, E. (1982). A patch-clamp study of bovine chromaffin cells and of their sensitivity to acetylcholine. *Journal of Physiology* **331**, 577–597.

FROMM, M. & SCHULTZ, S. G. (1981). Some properties of KCl-filled microelectrodes: correlation of potassium 'leakage' with tip resistance. *Journal of Membrane Biology* **62**, 239–244.

GUGGINO, W. B., LONDON, R. D., BOULPAEP, E. L. & GIEBISCH, G. (1983). Chloride transport across the basolateral cell membrane of the *Necturus* proximal tubule: dependence on bicarbonate and sodium. *Journal of Membrane Biology* **71**, 227–240.

HAMILL, O. P., MARTY, A., NEHER, E., SAKMANN, B. & SIGWORTH, F. J. (1981). Improved patch clamp techniques for high-resolution current recording from cells and cell-free membrane patches. *Pflügers Archiv* **391**, 85–100.

HAGIWARA, S. & TAKAHASHI, K. (1974). The anomalous rectification and cation selectivity of the membrane of a starfish egg. *Journal of Membrane Biology* **18**, 61–80.

HENKART, M. P. & NELSON, P. G. (1979). Evidence for an intracellular calcium store releasable by surface stimuli in fibroblasts (L cells). *Journal of General Physiology* **218**, 655–673.

HODGKIN, A. L. (1958). Ionic movements and electrical activity in giant nerve fibres. *Proceedings of the Royal Society* B **148**, 1–37.

HODGKIN, A. L. & KATZ, B. (1949). The effect of sodium ions on the electrical activity of the giant axon of the squid. *Journal of Physiology* **108**, 37–77.

HUME, J. R. & GILES, W. (1983). Ionic currents in single isolated bullfrog atrial cells. *Journal of General Physiology* **81**, 153–194.

JAYME, D. W., ADELBERG, E. A. & SLAYMAN, C. W. (1981). Reduction of K^+ efflux in cultured mouse fibroblasts, by mutation or by diuretics, permits growth in K^+-deficient medium. *Proceedings of the National Academy of Sciences of the U.S.A.* **78**, 1057–1061.

JENSEN, R. J. & DEVOE, R. D. (1983). Comparisons of directionally selective with other ganglion cells of the turtle retina: intracellular recording and staining. *Journal of Comparative Neurology* **217**, 271–287.

JOHNSTONE, R. M. (1978). The hyperpolarizing and depolarizing effects of 2,4-dinitrophenol on Ehrlich cells. *Biochimica et biophysica acta* **512**, 550–556.

KATZ, B. (1949). Les constantes électriques de la membrane du muscle. *Archives des sciences physiologiques* **3**, 285–300.

KRUEGER, B. K., FRENCH, R. J., BLAUSTEIN, M. B. & WORLEY, J. F. (1982). Incorporation of Ca-activated K-channel, from rat brain, into planar lipid bilayers. *Biophysical Journal* **37**, 170*a*.

LAMB, J. F. & MACKINNON, M. G. A. (1971*a*). Effect of ouabain and metabolic inhibitors on the Na and K movements and nucleotide contents of L cells. *Journal of Physiology* **213**, 665–687.

LAMB, J. F. & MACKINNON, M. G. A. (1971*b*). The membrane potential and permeabilities of the L-cell membrane to Na, K and chloride. *Journal of Physiology* **213**, 683–689.

LARIS, P. C., PERSHADSINGH, H. A. & JOHNSTONE, R. M. (1976). Monitoring membrane potentials in Ehrlich ascites tumor cells by means of a fluorescent dye. *Biochimica et biophysica acta* **436**, 475–488.

LASSEN, U. V. (1977). Membrane potential and conductance of the red cell membrane. *Membrane Transport in Red Cells*, ed. ELLORY, J. C. & LEW, V. L., pp. 137–172. London: Academic Press.

LASSEN, U. V., PAPE, L. & VESTERGAARD-BOGIND, B. (1978). Chloride conductance of the *Amphiuma* red cell membrane. *Journal of Membrane Biology* **39**, 27–48.

LATORRE, R., VERGARA, C. & HIDALGO, C. (1982). Reconstitution in planar lipid bilayers of Ca^{2+}-dependent K^+ channel from transverse tubule membranes isolated from rabbit skeletal muscle. *Proceedings of the National Academy of Sciences of the U.S.A.* **79**, 805–809.

LIBOFF, A. R. & RINALDI, R. A. (1974). (Eds.) Electrically mediated growth mechanisms in living systems. *Annals of the New York Academy of Sciences* **238**.

LINDEMANN, B. (1975). Impalement artifacts in microelectrode recordings of epithelial membrane potentials. *Biophysical Journal* **15**, 1161–1164.

LING, G. & GERARD, R. (1949). The normal membrane potential of frog sartorious fibers. *Journal of Cellular and Comparative Physiology* **34**, 383–396.

LUX, H. D. & BROWN, A. M. (1984). Patch and whole cell calcium currents recorded simultaneously in snail neurons. *Journal of General Physiology* **83**, 727–750.

MARQUARDT, D. W. (1963). An algorithm for least-squares estimation of non-linear parameters. *Journal of the Society for Industrial and Applied Mathematics* **11**, 431–441.

MARTY, A. (1981). Ca-dependent K channels with large unitary conductance in chromaffin cell membranes. *Nature* **291**, 497–500.

MARTY, A. & NEHER, E. (1984). Tight-seal whole-cell recording. In *Single-channel Recording*, ed. SAKMANN, B. & NEHER, E., pp. 107–122. New York: Plenum Press.

METHFESSEL, C. & BOHEIM, G. (1982). The gating of single calcium-dependent potassium channels is described by an activation/blockade mechanism. *Biophysics of Structure and Mechanism* **9**, 35–60.

NELSON, D. J., EHRENELD, J. & LINDEMANN, B. (1978). Volume changes and potential artifacts of epithelial cells of frog skin following impalement with microelectrodes filled with 3 M-KCl. *Journal of Membrane Biology*, Special Issue, 91–119.

NELSON, P. G., PEACOCK, J. & MINNA, J. (1972). An active electrical response in fibroblasts. *Journal of General Physiology* **60**, 58–71.

NOBLE, D. (1962). A modification of the Hodgkin–Huxley equations applicable to Purkinje fibre action and pacemaker potentials. *Journal of Physiology* **160**, 317–352.

NOBLE, D. & TSIEN, R. W. (1968). The kinetics and rectifier properties of the slow potassium current in cardiac Purkinje fibres. *Journal of Physiology* **195**, 185–214.

OKADA, Y., DOITA, Y., ROY, G., TSUCHIYA, W., INOUYE, K. & INOUYE, A. (1977). Oscillations of membrane potential in L cells. I. Basic characteristics. *Journal of Membrane Biology* **35**, 319–335.

OKADA, Y., TSUCHIYA, W. & INOUYE, A. (1979). Oscillations of membrane potential in L cells. IV. Role of intracellular Ca^{2+} in hyperpolarizing excitability. *Journal of Membrane Biology* **47**, 357–376.

OKADA, Y., TSUCHIYA, W. & YADA, T. (1982). Calcium channel and calcium pump involved in oscillatory hyperpolarizing responses of L-strain mouse fibroblasts. *Journal of Physiology* **327**, 449–461.

OSTERHOUT, W. J. V. (1925). On the importance of maintaining certain differences between cell sap and external medium. *Journal of General Physiology* **7**, 561–564.

PAGE, K. R., KELDAY, L. S. & BOWLING, D. J. F. (1981). The diffusion of KCl from microelectrodes. *Journal of Experimental Botany* **32**, 55–58.

PALLOTTA, B. S., MAGLEBY, K. L. & BARRETT, J. N. (1981). Single channel recordings of Ca^{2+}-activated K^+ currents in rat muscle cell culture. *Nature* **293**, 471–474.

PIWNICA-WORMS, D., JACOB, R., HORRES, R. & LIEBERMAN, M. (1983). Transmembrane chloride flux in tissue-cultured heart cells. *Journal of General Physiology* **81**, 731–748.

PRICE, P. G. (1970). Electron microscopic observations of the surface of L-cells in culture. *Journal of Membrane Biology* **2**, 300–316.

ROY, G. & OKADA, Y. (1978). Oscillation of membrane potential in L cells: III. K current–voltage curves. *Journal of Membrane Biology* **38**, 347–357.

ROY, G. & SAUVE, R. (1983). Stable membrane potentials and mechanical K^+ responses activated by internal Ca^{2+} in HeLa cells. *Canadian Journal of Physiology and Pharmacology* **61**, 144–148.

SANFORD, K. K., EARLE, W. R. & LIKELY, G. D. (1948). The growth *in vitro* of single isolated tissue cells. *Journal of the National Cancer Institute* **9**, 229–246.

SHERBET, G. V. (1978). Bioelectric potentials and the cell surface. *The Biophysical Characterization of the Cell Surface*, chap. 3, pp. 14–36. New York: Academic Press.

SHINDO, T. & SPRING, K. R. (1981). Chloride movement across the basolateral membrane of proximal tubule cells. *Journal of Membrane Biology* **58**, 35–42.

STANNERS, C. P., ELICEIRI, G. L. & GREEN, H. (1971). Two types of ribosome in mouse–hamster hybrid cells. *Nature New Biology* **230**, 52–54.

VERGARA, C. & LATORRE, R. (1983). Kinetics of Ca^{2+}-activated K^+ channels from rabbit muscle incorporated into planar bilayers. Evidence for a Ca^{2+} and Ba^{2+} blockade. *Journal of General Physiology* **82**, 543–568.

WONG, B. S., LECAR, H. & ADLER, M. (1982). Single calcium-dependent potassium channels in clonal anterior pituitary cells. *Biophysical Journal* **39**, 313–317.

YELLEN, G. (1982). Single Ca^{2+}-activated nonselective cation channels in neuroblastoma. *Nature* **296**, 357–359.